Decomposed-Components Approach to Signal-Pole Base-Plate Design

GONGKANG FU, SHERIF J. BOULOS, DENIZ SANDHU, AND SREENIVAS ALAMPALLI

The AASHTO specification does not specify the analysis method for base-plate design of span-wire traffic signal poles. The study reported here consisted of full-scale testing and finite element analysis of a number of existing signal poles to examine their behavior and evaluate their structural adequacy. A simplified analysis method has been developed because present procedures were found to be unreliable. This method is consistent with the working stress design concept in the current code. It decomposes the base plate into three elementary components corresponding to three critical regions of maximum stress. The subsequent analyses become straightforward on the basis of these modelings, with the assistance of empirically determined coefficients to reach equivalent section capacities with respect to critical stresses. Hand calculation is adequate for applications of this method in routine design.

Traffic-signal poles that are span-wire mounted (referred to here simply as "signal poles") currently are designed according to the AASHTO specification (*1*). Provisions are given for analysis and design of the post and anchor bolts, but no method is specified for analysis of the base plate. This study examined structural adequacy of the base plates of signal poles supplied to New York State. As a result, a semiempirical method was developed for analyzing base plates because the current procedures were found to be unreliable. This method is intended to be consistent with the working stress design adopted by the current code and may be included in the specification for design applications.

In New York State, a typical signal pole consists of a round or polygonal steel post with changing diameter welded to a square steel base plate. The base plate is anchored to a concrete footing by four bolts. A reinforced hand hole is provided in the post. Typical pole details are shown in Figure 1. Dead, wind, and ice loads are required to be covered in pole design (*1,2*). Their combinations and corresponding strength requirements are provided by the code (*1*). In this paper signal poles are identified by the first letter of the manufacturer's name, design load in kips, and height in feet. For example, C530 is a pole manufactured by Carlan Manufacturing Company, with a design load of 22.2 kN (5 kips), that is 9.14 m (30 ft) tall. Two critical loadings are considered here: parallel loading, in which the wire runs parallel to a side of the square base plate, and diagonal loading, in which the wire runs along a diagonal of the base plate.

Full-scale load tests and material tests were performed to investigate signal pole behaviors under loading. Finite element analysis (FEA) models were developed and verified by the test results. Typical areas of critical stress concentration in the base plate were identified. Simple models based on decomposed elementary components were developed for each critical case, with corresponding loads. Analysis of these critical cases can thus be simplified, with assistance of empirical coefficients to reach equivalent capacities with respect to critical stresses. These coefficients were determined by FEA for 23 representative signal poles and 5 inadequate ones that were redesigned.

Engineering Research and Development Bureau, State Campus, New York State Department of Transportation, Albany, N.Y. 12232.

TEST PROGRAM AND FEA

Three poles were instrumented with electrical resistance strain gauges and load tested. Two (C530 and C832) were from the manufacturer's standard stock. The third, C530(T), was specially built with a thinner base plate than the standard C530 pole, to examine the effect of this thickness on the behavior and strength of the base plate. Their dimensions are detailed in Table 1. They were selected to include various base plate thicknesses and clearances between the bolt circle diameter (BC) and the pole diameter at its bottom (DB). These were initially considered important factors affecting stress distribution in the base plate.

Test setup details are shown in Figure 2. All poles tested were individually anchored horizontally to a foundation. Figures 3, 4, and 5 show strain gauge identifications and locations on the post, base plate, and anchor bolts. Loads were applied laterally to each pole at 457 mm (18 in.) from its tip (where the span wire is mounted in service condition) by a hydraulic jack. Applied load levels were measured by a pressure gauge with a resolution of 0.995 kN (223.6 lb) [i.e., 690 kPa (100 psi) on a cylinder area of 0.00144 m^2 (2.236 $in.^2$)]. The poles were subjected to either diagonal or parallel loading by rotating them about their central axes without changing the direction of load (Figure 2). No concrete packing was provided between the base plate and the steel test foundation (Figure 2) as would be the case in a critical—even if temporary—service condition.

After the load tests, samples were taken from each standard pole's post, base plate, and anchor bolts for material laboratory tests; the results are given in Table 2. A second sample from the C832 base plate was tested after the first showed an unexpectedly low strength, which was thus confirmed.

Load test results and FEA predictions will now be discussed. For simplicity of presentation, the structural response obtained in strain has been converted to stress according to

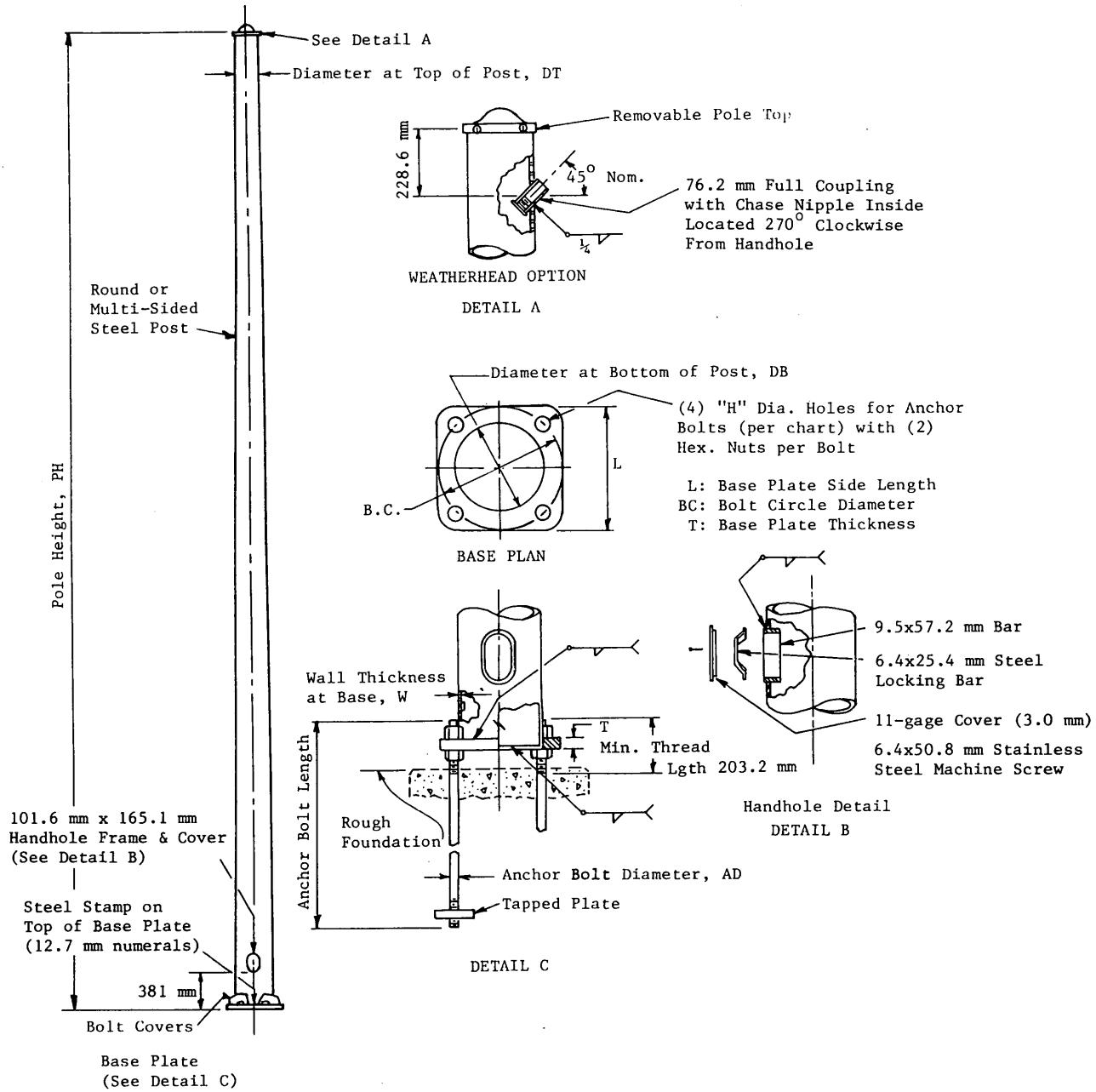

FIGURE 1 Typical traffic-signal pole in New York.

TABLE 1 Dimension Details of Tested Signal Poles

Pole ID	C530(T)	C530	C832
Pole Height (PH), m	9.14	9.14	9.75
Design Load, kN	22.2	22.2	22.2
Diameter at Top of Post (DT), mm	273	273	324
Diameter at Bottom of Post (DB), mm	324	324	406
Wall Thickness of Post at Base (W), mm	7.94	7.94	9.53
Base Plate Side Length (L), mm	584	584	559
Base Plate Thickness (T), mm	31.8	44.4	57.2
Bolt Circle Diameter (BC), mm	584	584	559
Anchor Bolt Diameter (AD), mm	38.1	38.1	50.8

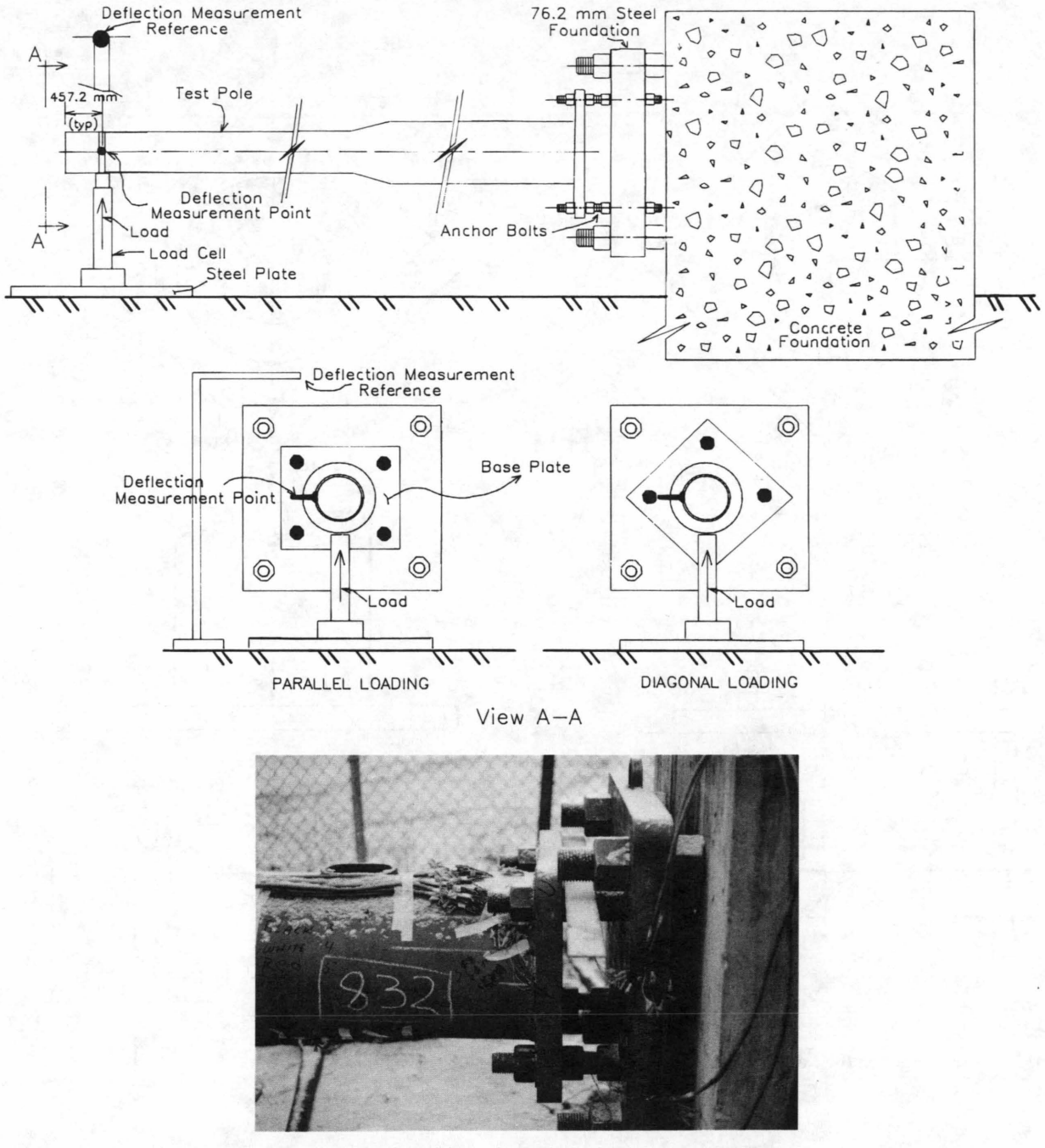

FIGURE 2 Load test setup (not to scale).

the elastic stress-strain constitutive relation, although it is obviously not valid in inelastic ranges. The FEA was performed using Graphics Interactive Finite Element Total System (GIFTS) software (*3*). This analysis was limited to the elastic range. Two quarter models were generated to analyze the poles under the diagonal and parallel loading, taking into account their symmetric and antisymmetric behaviors. The post was modeled by a combination of plate elements (for the top part) and solid elements (for the bottom part near the base). The base plate was modeled by multiple layers of solid elements. The anchor bolts were modeled by beam elements.

Load Test A

Pole C530(T) was loaded diagonally to failure, with the instrumentation shown in Figure 3. Two load cycles were applied up to loads of 17.9 kN (4,025 lb) and 20.5 kN (4,616 lb), respectively. Figure 6 shows the stress response of the base plate to the loads. Only the dominant component S_y (bending stress in the y direction) of Gauge R12 is included, showing the maximum response. The FEA predicted virtually the same stress shown by the strain gauge, within the elastic range. Note that the inelastic behavior under higher loads shown in Figure 6 was initiated in an anchor bolt (*4*). In

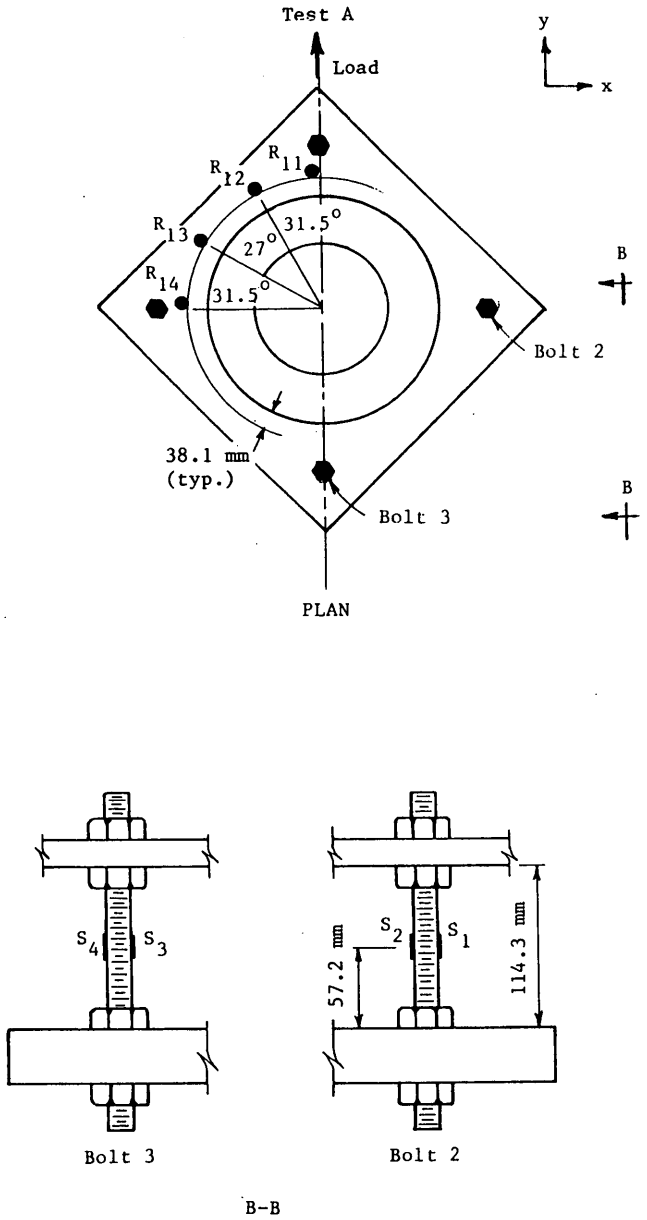

FIGURE 3 Instrumentation for Load Test A: C530(T).

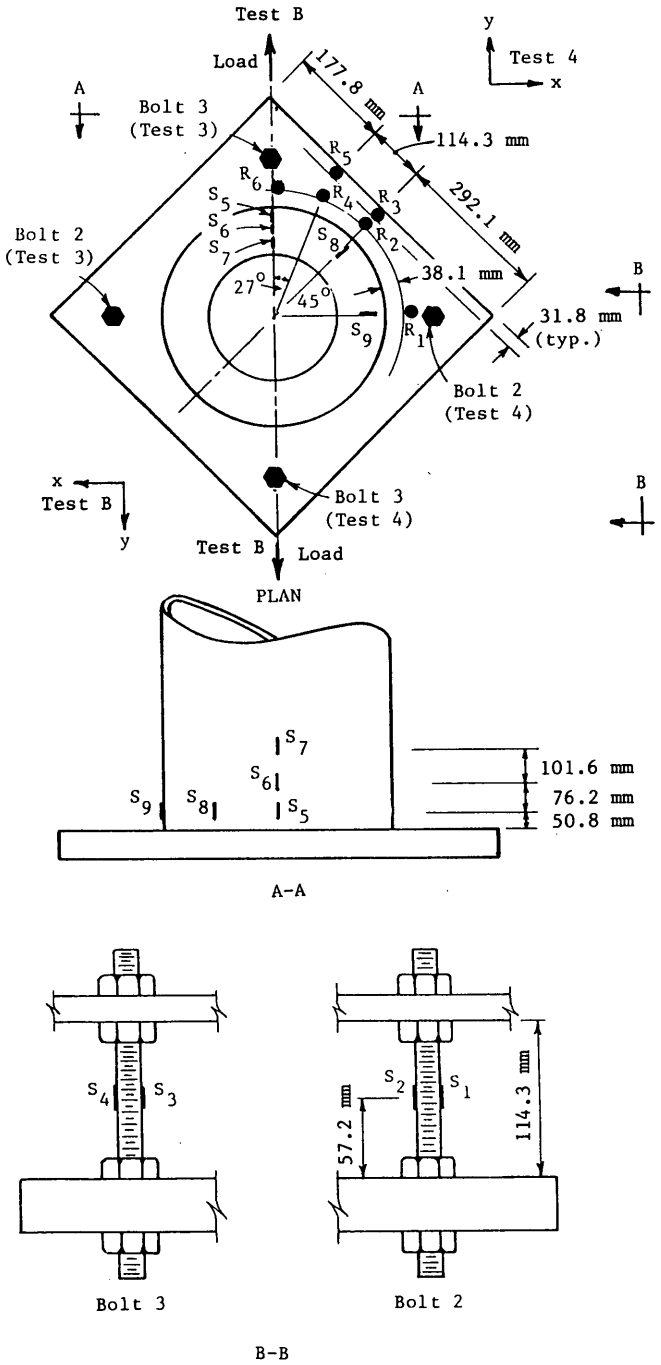

FIGURE 4 Instrumentation for Load Test B: C530.

addition, by linear extrapolation of the first (elastic) part of the load-stress relation in Figure 6, the base plate was also a deficient component of the pole because of its reduced thickness. The base plate showed residual deformation in the area between Gauges R12 and R13 as well as its symmetric counterpart, which was apparently associated with the maximum stress discussed earlier.

Load Test B

Pole C530 was subjected to diagonal loading with strain gauges on the post observing tensile strains (Figure 4). It was loaded successively up to 10.9 and 12.9 kN (2,460 and 2,907 lb) in two cycles. Among the strain gauges on the base plate, R4 showed the highest stress level. Its dominant component S_y is shown in Figure 7. The FEA result is in good agreement within the elastic range with that of the testing. Inelastic behavior of the pole was caused by partial yielding of an anchor bolt, a result similar to that in Load Test A (*4*). By linear extrapolation of the elastic part of its load-stress relation, the base plate also was found to be deficient. The same pole was load-tested again under a diagonal load after being turned

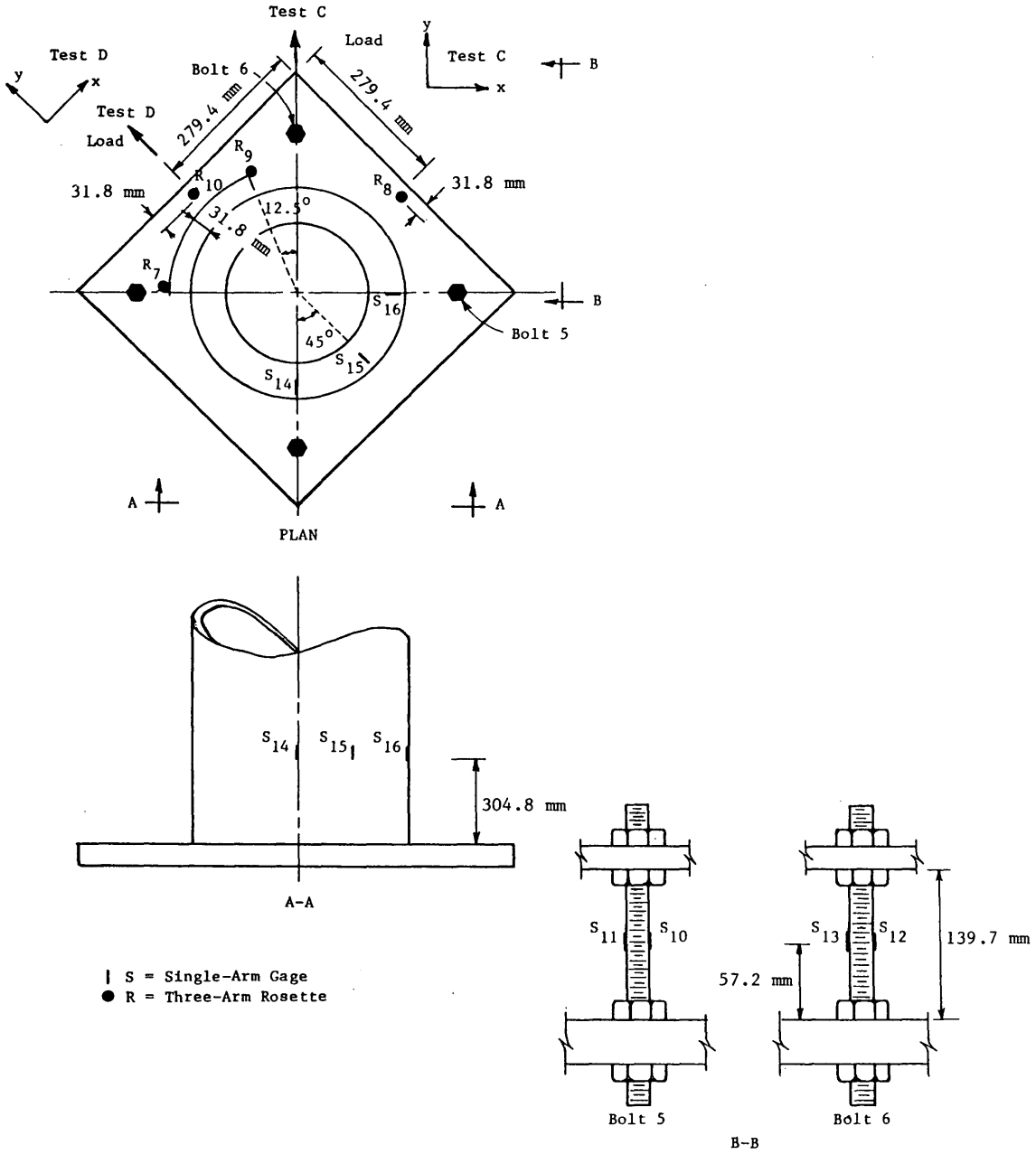

FIGURE 5 Instrumentation for Load Tests C and D: C832.

TABLE 2 Material Coupon Test Results

Sample	Steel Type	Nominal Yield, MPa	2% Yield Strength, MPa	Ultimate Strength, MPa
POLE C530				
Post	A 252	345	375	490
Plate	A 36	248	256	436
Bolt	A 366 M 55	379	417	611
POLE C832				
Post	A 53	345	326	489
Plate*	A 36	248	194	310
	A 36	248	200	304
Bolt	A 36 M 55	379	405	595

*Second sample tested for verification.

180 degrees about its central axis. Similar results were obtained, and the assumed symmetry was verified (*4*).

Load Test C

Pole C832 was first loaded diagonally, with the strain gauges on the post under tension (Figure 5). The pole was loaded up to 25.9 and 31.8 kN (5,814 and 7,155 lb) in two successive cycles. Among the base plate strain gauges, R8 and R10 showed the highest stress levels symmetrically. Figure 8 shows load-stress curves for R10; only the dominant (bending and shear) components are included. The validity of the FEA models for the elastic range is again demonstrated. Residual strains were observed at the ends of both cycles. Yielding was initiated at a load between 20.9 and 25.9 kN (4,696 and 5,814 lb) at an anchor bolt (*4*).

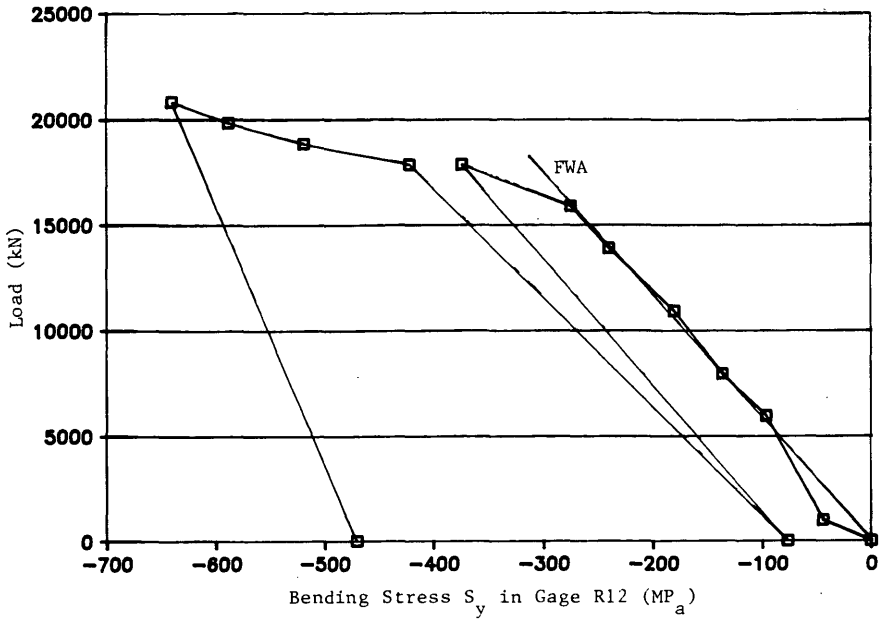

FIGURE 6 Load Test A: C530(T) under diagonal load.

Load Test D

Pole C832 was reset for parallel loading (Figure 5) and loaded through five cycles. Among the base-plate strain gauges, R8 and R10 showed the highest stress levels. Figure 9 shows load-stress curves of their respective dominant components. FEA again predicted these stresses fairly accurately. Inelastic behavior under higher loads shown in these figures was initiated in an anchor bolt, although the maximum stress level was much lower than that in Load Test C (*4*). This shows, as expected, that the diagonal load is the governing loading case for the anchor bolts, which appears to have been ignored in the design of these poles.

Table 3 gives a numerical comparison of test and FEA results of C832 (Load Test C) as a typical case including nondominant components of stresses. These results are shown to be consistent with one another, especially for the pronounced stresses indicating critical response to the load. Relatively larger differences between FEA and test results (for example, in R7) are attributed to inevitable discrepancies between the location of a strain gauge and its corresponding element in FEA or higher noise-to-signal ratios in the acqui-

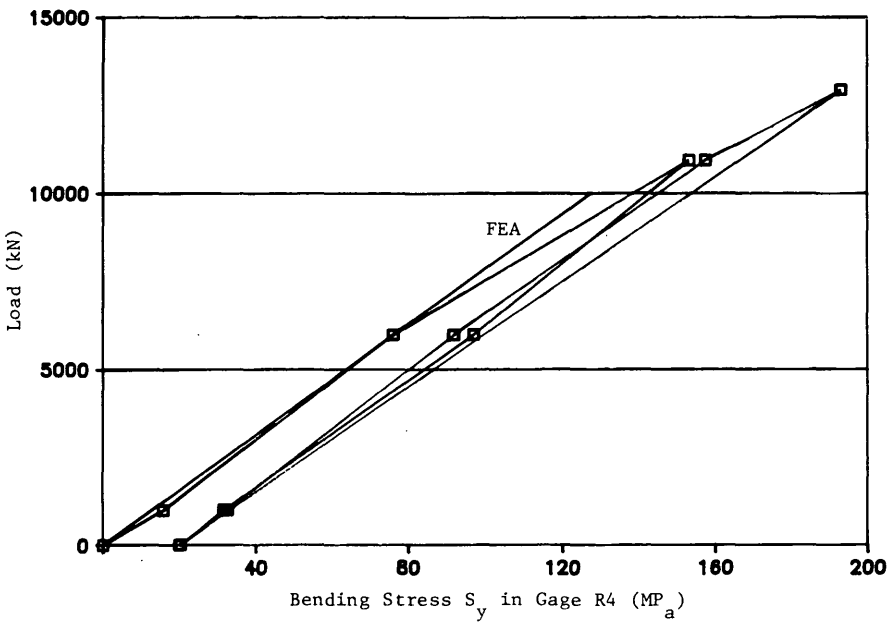

FIGURE 7 Load Test B: C530 under diagonal load.

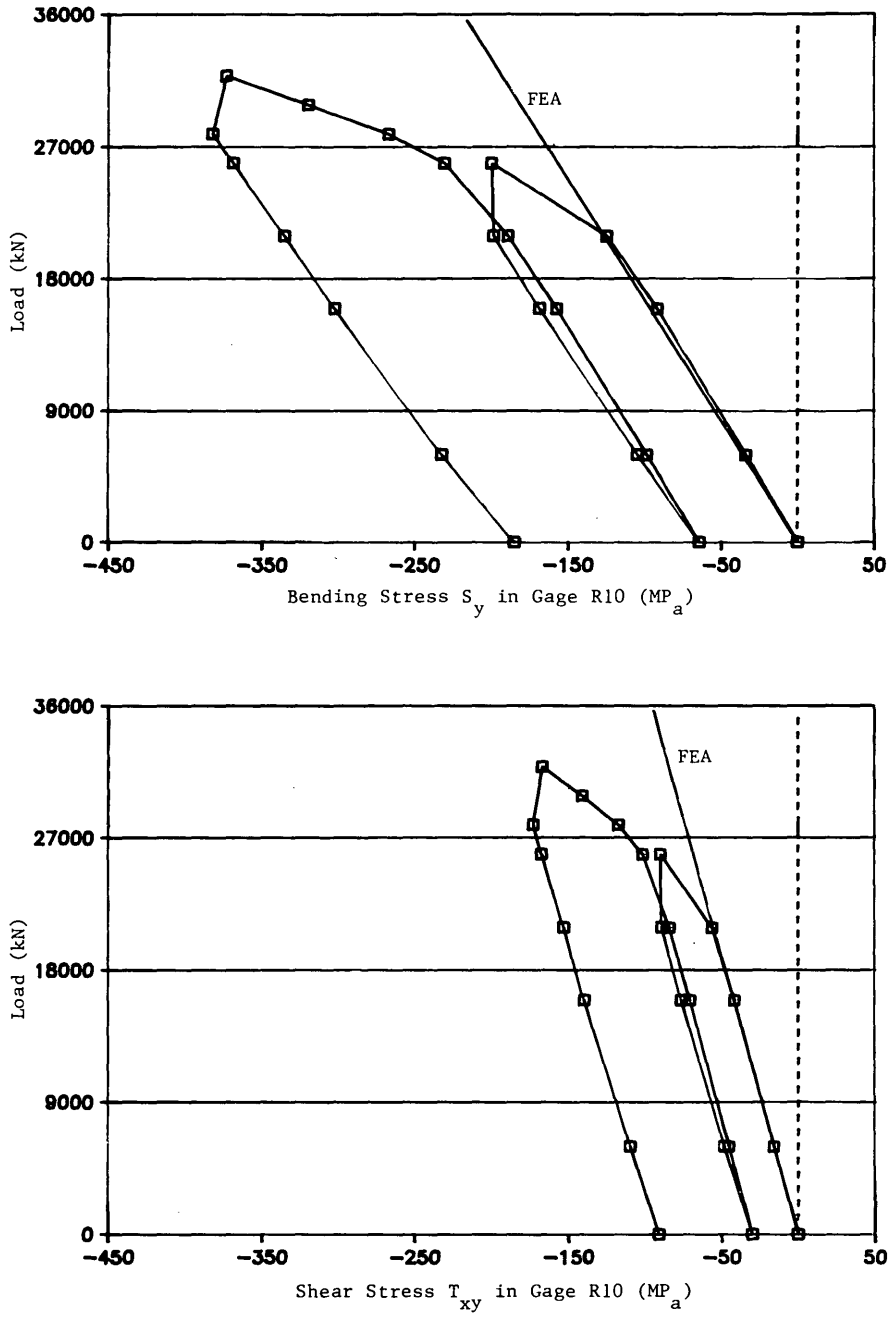

FIGURE 8 Load Test C: C832 under diagonal load: (*top*) bending stress, (*bottom*) shear stress.

sition of test data, or both, when the strain signal was low. Good agreement between FEA and test results was also observed for tip deflections and stresses on the post and in the anchor bolts (*4*). This agreement also verified the beam assumption adopted by the current AASHTO code.

BASE-PLATE BEHAVIOR AND DECOMPOSED-COMPONENTS METHOD FOR ANALYSIS

Figure 10 shows typical deflection distribution and stress contours of the top surface of a base plate under diagonal loading as obtained by FEA for the design load. Stress is expressed as the percentage of overstress using the Von Mises criterion against the pole's nominal yield stress F_y = 248 MPa (36 ksi). The shaded area is a critical region (120 and 130 percent of F_y), obviously associated with the deflection described. Figure 11 shows another typical case of behavior under parallel loading. Stress contours again are expressed by overstress percentage using the same criterion as in Figure 10. Two shaded areas are identified as critical regions. It is interesting that they represent maximum stresses under the given load contributed by the dominant bending component (S_x in Region B) and shear component (T_{xy} in Region C). Figure 12 shows

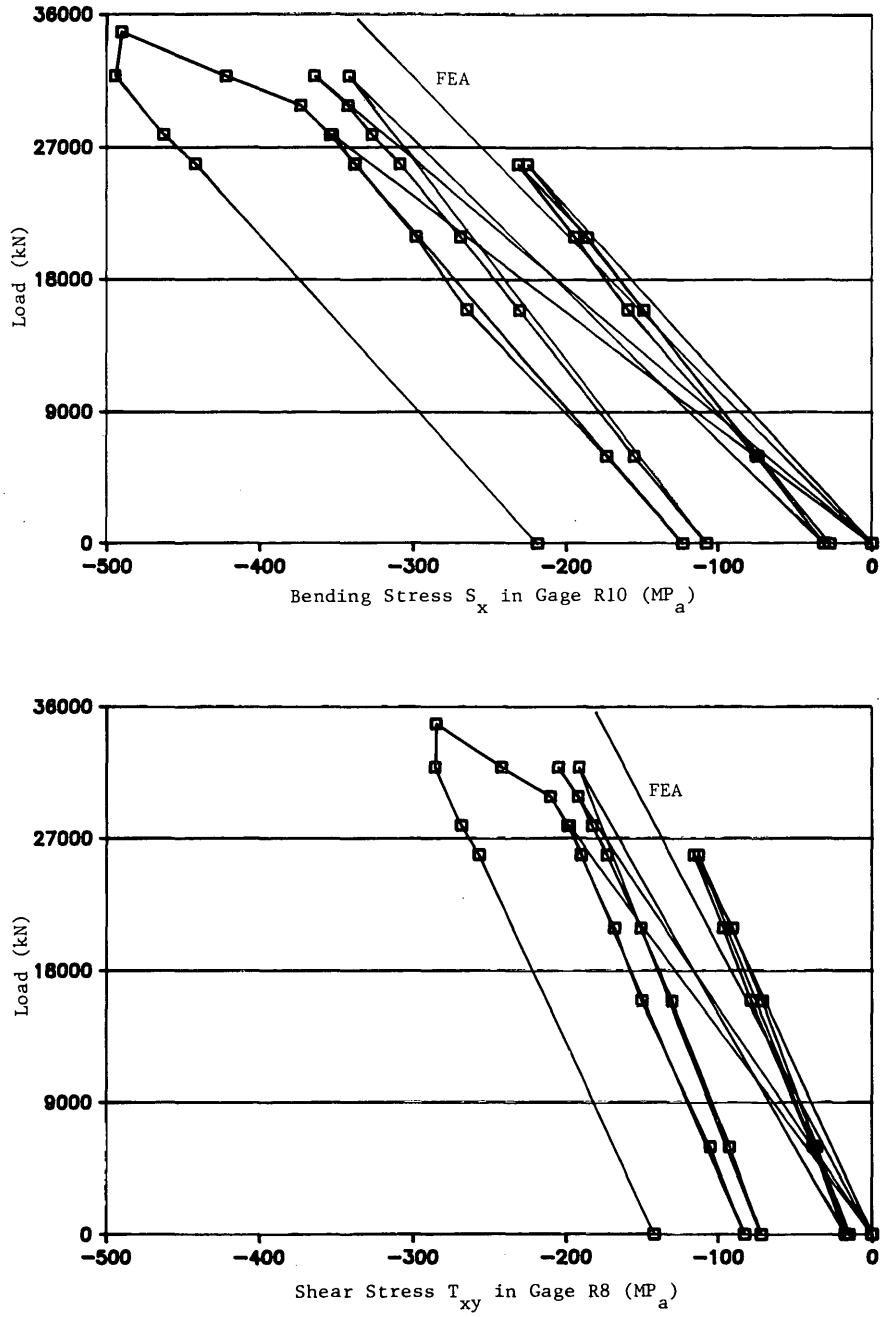

FIGURE 9 Load Test D: C832 under parallel load: (*top*) bending stress, (*bottom*) shear stress.

TABLE 3 Numerical Comparison of Testing and FEA Results in Base Plate Stress (Pole C832 in Load Test C Under Diagonal 15.9-kN Load)

Strain Gage ID	Stress Components, MPa						Dominant Stress Component	Difference In Dominant Stress Component, %
	Test			FEA				
	Sx	Sy	Txy	Sx	Sy	Txy		
R7	+3.65	-3.65	+27.7	+1.86	-9.31	+32.6	Txy	+17.7
R8	+1.79	-91.0	+41.4	+2.21	-90.9	+43.2	Sy	+0.1
R9	-13.7	-34.5	-54.1	-15.4	-53.6	-56.5	Txy	+4.5
R10	+1.59	-91.2	-41.4	+2.21	-90.9	-43.2	Sy	+0.2

NOTE: See Figure 5 for loading and gage locations.

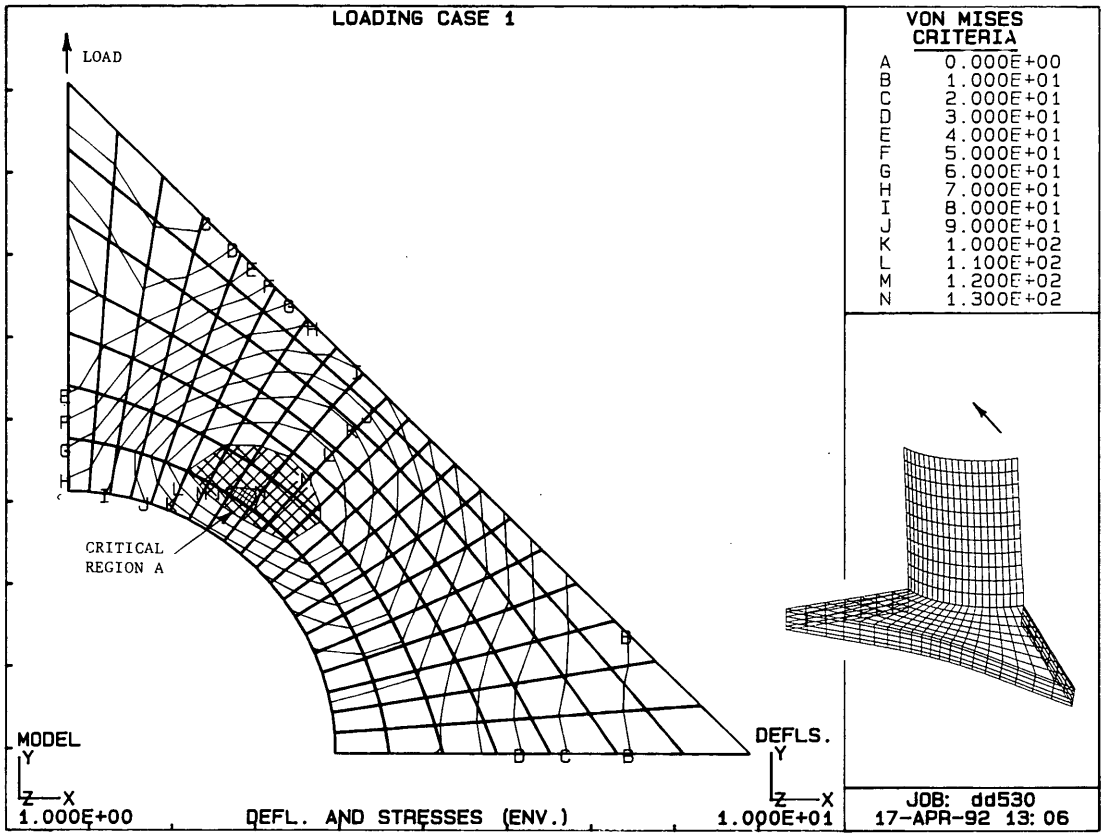

FIGURE 10 Typical deflection and stress distribution under diagonal load (C530, 22.2 kN).

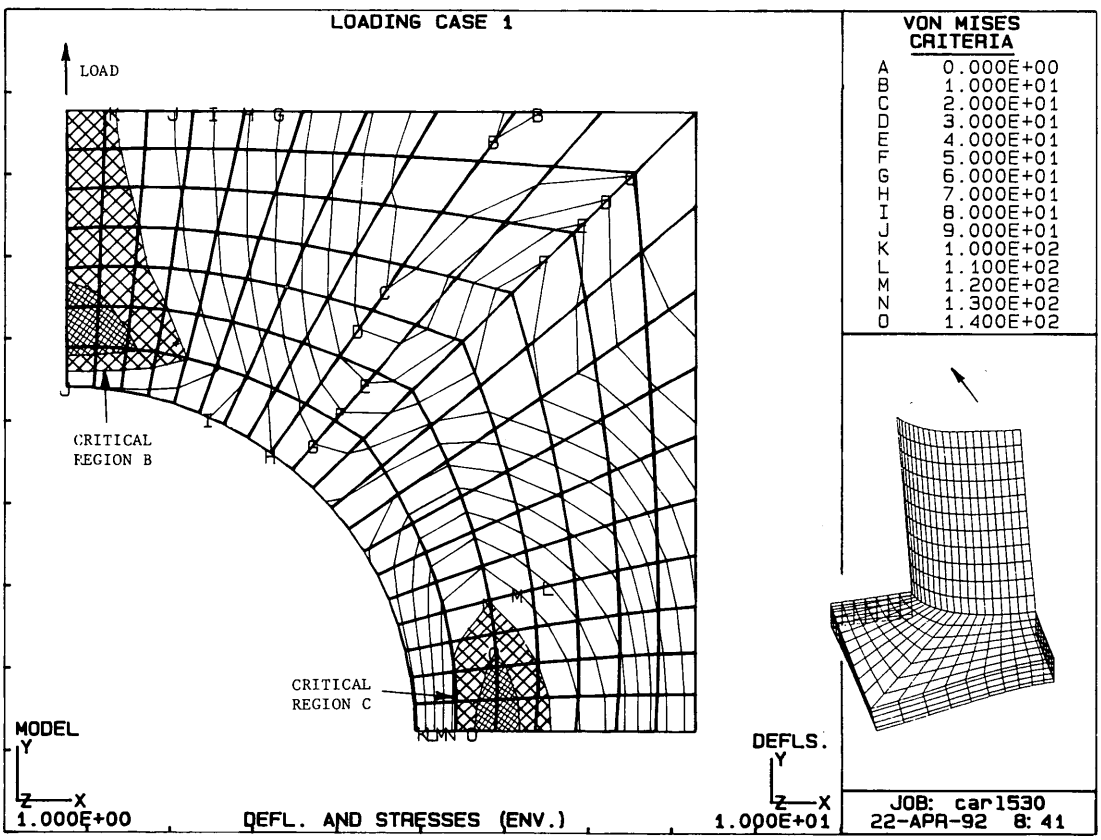

FIGURE 11 Typical deflection and stress distribution under parallel load (C530, 22.2 kN).

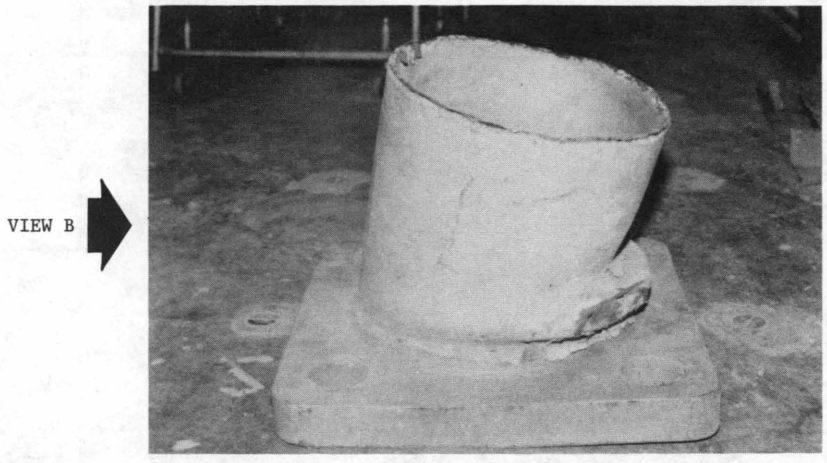

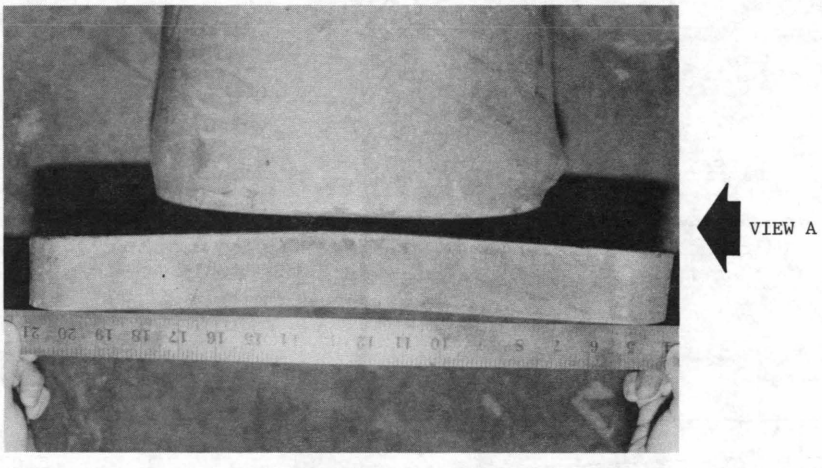

FIGURE 12 Actual residual deflection resulting from parallel loading in an accident.

the true deflection distribution of an accidental failure. This incident occurred under parallel loading when a truck snagged a span wire in service. The three critical regions indicated in Figures 10–12 are thus addressed in the suggested new analysis method for the base plate.

This method of analysis uses the concept of decomposed components for simplification. For each potential failure mode (or critical region), a part of the base plate is isolated and modeled by an elementary component (e.g., a beam or bar). Then a critical cross section and the corresponding load are identified. The subsequent analysis thus becomes straightforward, with the assistance of an empirical coefficient modifying the section's elastic capacity to reach an equivalent section modulus with respect to the maximum stress. These equivalent coefficients were determined empirically by considering 23 representative signal poles designed by three major New York State suppliers and 5 inadequate poles that were redesigned; the dimensions are given in Table 4.

This method is intended to be consistent with the current working stress design concept adopted by the AASHTO code with respect to strength requirements, to obtain critical stresses within the elastic range. The resulting stresses are to be used to meet the AASHTO strength requirements:

$$f_b \leq kF_b \qquad f_v \leq kF_v \tag{1}$$

where

k = value given by the current AASHTO code—for example, 1.4 for Group II load;
F = allowable stress;
f = computed stress; and
b and v = subscripts for bending and shear stresses, respectively.

All three critical stresses must be considered for proportioning.

TABLE 4 Dimension Details of Sample Poles

Pole ID	Post Dimensions, mm DT	DB	w	Base Plate Dimensions, mm L	T	BC	Anchor Dimensions, mm AD
EXISTING POLES							
C326	219	273	6.35	432	38.1	432	31.8
C328	219	273	6.35	457	38.1	457	31.8
C430	273	324	7.11	457	44.5	457	38.1
C530	273	324	7.94	584	44.5	584	38.1
C530'	273	324	7.94	457	50.8	457	44.5
C732	324	406	7.94	635	63.5	635	38.1
C832	324	406	9.53	559	57.2	559	50.8
S324	178	254	4.76	533	38.1	533	38.1
S328	191	279	4.76	533	38.1	533	38.1
S334	216	330	4.76	686	38.1	635	38.1
S434	241	356	4.76	686	44.5	635	44.5
S530	267	368	4.76	686	44.5	635	44.5
S632	305	419	4.76	686	50.8	737	50.8
S832	381	483	4.76	813	57.2	813	50.8
S934	419	533	4.76	838	57.2	851	57.2
S1036	445	572	4.76	889	57.2	851	57.2
U226	174	267	4.55	358	38.1	356	31.8
U530	249	356	6.35	521	50.8	508	44.5
U636	297	425	6.35	660	50.8	597	44.5
U832	305	419	7.94	622	63.5	597	50.8
U840	279	470	7.94	660	63.5	635	57.2
U1040	391	533	7.94	699	69.9	699	57.2
U1044	401	546	7.94	737	69.9	711	57.2
REDESIGN CASES							
632	305	419	4.76	686	57.2	737	50.8
934a	419	533	4.76	838	69.9	851	57.2
934b	419	533	4.76	838	76.2	851	57.2
226	174	267	4.55	358	44.5	356	31.8
1040	401	546	7.94	737	82.6	711	57.2

Dimensions (Fig. 1): DT = diameter at top of post, DB = diameter at bottom of post, w = wall thickness at its base, L = side length of square base plate, T = thickness of base plate, BC = bolt circle diameter, AD = anchor bolt diameter.

Bending stress due to diagonal load (for Critical Region A in Figure 10) is

f_b = anchor force * moment arm/equivalent flexural elastic section modulus

$$= \frac{M}{BC} * \frac{BC - DB}{2} \Big/ \{\alpha(1.414L - DB)T^2/6\} \tag{2a}$$

where M is the moment at the post base due to the design load and α is an empirical coefficient for an equivalent section modulus in terms of the critical stress:

$$\alpha = \{4.304 - 0.02021BC/T - 4.304DB/L + 4.503(DB/L)^2 - 0.9750(L - 0.707BC)/(L - DB) - 1.686BC/L\}/C_\alpha \tag{2b}$$

$$C_\alpha = 1.097 \tag{2c}$$

Equations 2a, 2b, and 2c are obtained by simplifying the problem as a cantilever beam under a concentrated load at its free end applied by an anchor bolt, as shown in Figure 13. This assumes that the critical point being checked is in Section S_a.

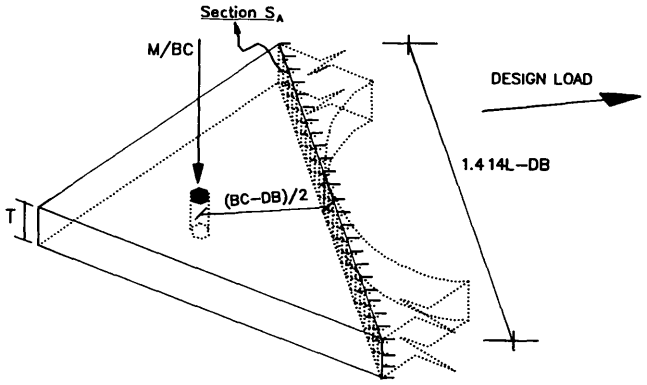

FIGURE 13 Simplified analysis model for maximum bending stress under diagonal load.

Bending stress due to parallel loading (for Critical Region B in Figure 11) is

f_b = midspan (maximum) moment/equivalent elastic flexural section modulus

$$= \frac{M}{4(DB/L')^2}\{1/4 - (1 - DB/L')/3 + (1 - DB/L')^4/12\}/\{\beta(L - DB)T^2/12\} \tag{3a}$$

where $L' = \max\{0.707BC, DB\}$ (max{ } means the maximum value of), and β is an empirically determined coefficient for an equivalent section modulus with respect to the critical stress:

$$\beta = \{157.6 - 21.85L/DB - 0.3300BC/T - 259.3DB/L - 48.13(L * T/DB/(L - DB))^{1/2} + 194.6(DB/L)^2 + 127.4T/BC - 21.65DB/BC\}/C_\beta \tag{3b}$$

$$C_\beta = 1.080 \tag{3c}$$

This case is treated as a beam with both ends built in and a span of $0.707BC$ under a triangularly distributed load applied by the post, as shown in Figure 14. Equation 3a checks a critical point on Section S_b.

Shear stress due to parallel loading (for Critical Region C in Figure 11) is

f_v = torque by anchors/equivalent elastic torsional section modulus

$$= \frac{M}{2} \Big/ \{\gamma C' b T^2\} \tag{4a}$$

where

$M/2$ = torque induced by anchor forces on the post base, which in turn is due to the design load;

b = $\min\{0.707BC, DB\}$ (min{ } means the minimum value of);

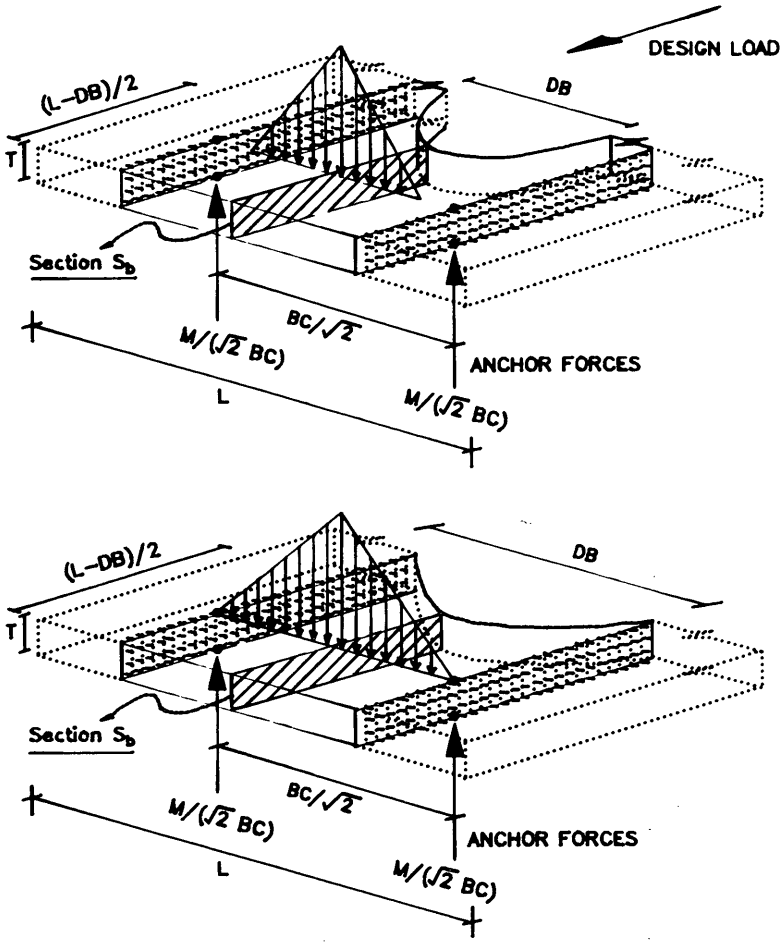

FIGURE 14 Simplified model for maximum bending stress under parallel load.

C' = coefficient given in Table 5 based on the elasticity solution, depending on the ratio b/T (*5*); and

γ = empirical coefficient to reach an equivalent cross section for prediction of critical stress:

$$\gamma = \{210.0 - 66.9BC/DB - 0.1719(BC - DB)/T - 714.8DB/L + 358.3(DB/L)^2 - 48.16(L - 0.707BC)/(L - DB) - 288.2(BC - DB)/(1.414L - DB) + 381.0BC/L\}/C_\gamma \quad (4b)$$

$$C_\gamma = 1.094 \quad (4c)$$

TABLE 5 Coefficient C' for Torsion (*4*)

b/T	C'	b/T	C'
1.0	0.208	3.0	0.267
1.2	0.219	4.0	0.282
1.5	0.231	5.0	0.291
2.0	0.246	10.0	0.312
2.5	0.258	∞	0.333

Equations 4a, 4b, and 4c are based on a simplification of the problem that considers a rectangular bar under torque $M/2$ applied by a pair of anchor bolts, as shown in Figure 15. The maximum shear stress occurs on Section S_c.

Figures 16–18 show the comparison of calculated stresses f by the suggested method and f_{FEA} by FEA for the three critical stress cases. The conservatism (overestimation) in f observed there is introduced by an amplification factor C_i =

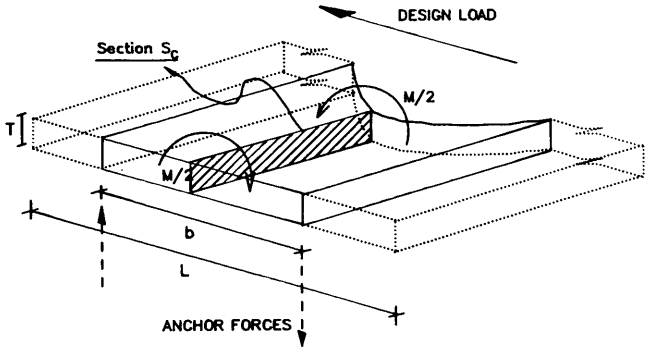

FIGURE 15 Simplified model for maximum shear stress under parallel load.

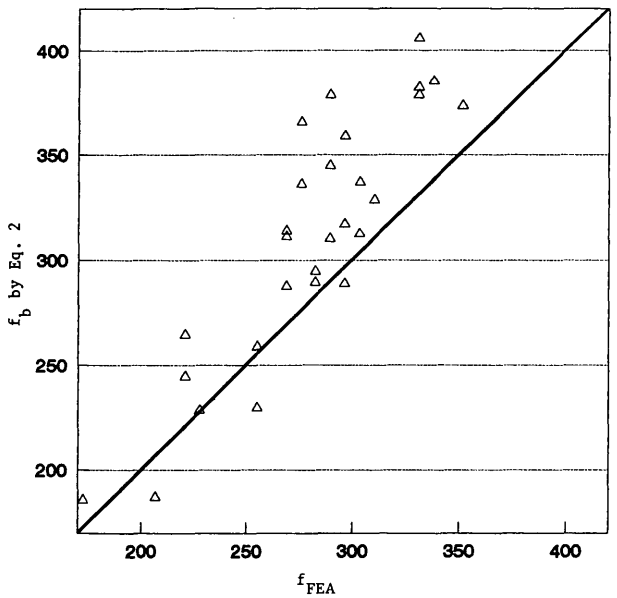

FIGURE 16 Comparison of critical stresses (MPa) by FEA and proposed method: bending under diagonal load.

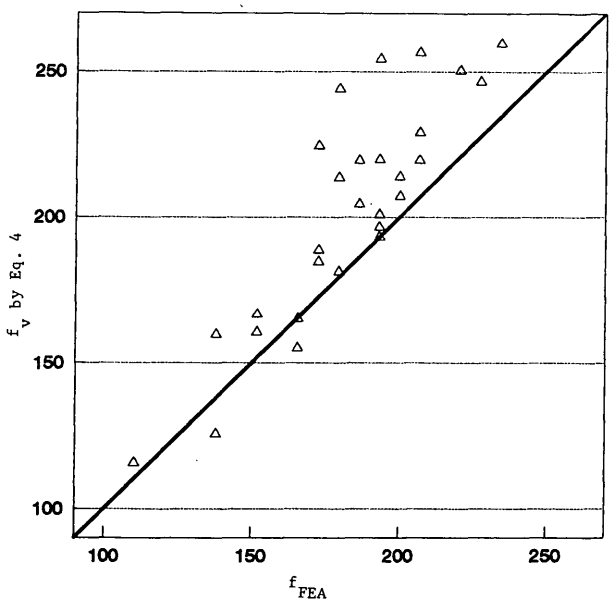

FIGURE 18 Comparison of critical stresses (MPa) by FEA and proposed method: shear under parallel load.

$m_i + \sigma_i$ ($i = \alpha, \beta, \gamma$), where $m_i(m_i + \sigma_i)$ and $\sigma_i(m_i + \sigma_i)$ are, respectively, the mean and the standard deviation of f/f_{FEA} for respective cases of critical stresses. m_i is around 1.0 and σ_i is about 0.090 for each case.

ILLUSTRATIVE EXAMPLE

The suggested analysis method is applied here to Pole S632 for its evaluation and modification as an example. F_y = 345 MPa (50 ksi) is used for proportioning; kF_b = 1.4 * 0.66 * 345 = 0.924 * 345 = 319 MPa (46.2 ksi) and kF_v = 1.4 * 0.4 * 345 = 0.56 * 345 = 193 MPa (28 ksi) are assumed for Load Groups II and III.

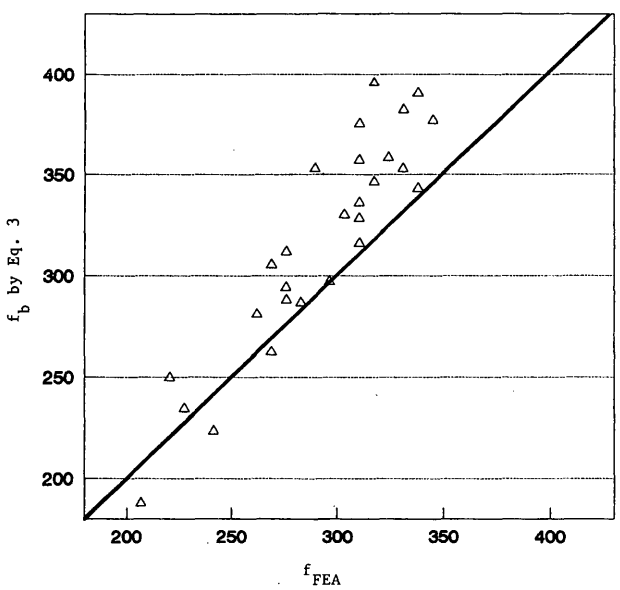

FIGURE 17 Comparison of critical stresses (MPa) by FEA and proposed method: bending under parallel load.

Step 1

From Table 4, L = 686 mm (27 in.), T = 50.8 mm (2 in.), BC = 737 mm (29 in.), and DB = 419 mm (16.50 in.). By definition, the pole is 9.75 m (32 ft) high and its design load is 26.7 kN (6 kips).

For maximum bending stress under diagonal loading,

Anchor force
= 6 * (32 − 1.5) * 12/29(4.448) = 337 kN (75.7 kips)
Moment arm = 0.5 * (29 − 16.5)(25.4) = 159 mm (6.25 in.)
Equivalent coefficient α
= {4.304 − 0.02021(29/2) − 4.304(16.5/27) + 4.503(16.5/27)^2 − 0.9750[27 − 0.707(29)]/(27 − 16.5) − 1.686(29/27)}/1.097 = 0.5909
Equivalent section modulus
= 0.5909(1.414 * 27 − 16.5)2^2/6(25.4)^3 = 140 × 10^3 mm^3 (8.541 in.^{3})
Maximum bending stress
= 75.7 * 6.25/8.541(6.90) = 382 MPa (55.4 ksi) > 319 MPa (46.2 ksi) NG.

Step 2

Increase the thickness T by 6 mm (0.25 in.): L = 686 mm (27 in.), T = 57 mm (2.25 in.), BC = 737 mm (29 in.), and DB = 419 mm (16.50 in.).

For maximum bending stress under diagonal loading,

Anchor force = 337 kN (75.7 kips)
Moment arm = 159 mm (6.25 in.)
Equivalent coefficient α
= {4.304 − 0.02021(29/2.25) − 4.304(16.5/27) + 4.503(16.5/27)^2 − 0.9750[27 − 0.707(29)]/(27 − 16.5) − 1.686(29/27)}/1.097 = 0.6206
Equivalent section modulus
= 0.6206(1.414 * 27 − 16.5)2.25^2/6(25.4)^3 = 186 × 10^3 mm^3 (11.35 in.^{3}).
Maximum bending stress
= 75.72(6.25)/11.35(6.90) = 288 MPa (41.7 ksi) < 319 MPa (46.2 ksi) OK.

For maximum bending stress under parallel loading,

M = 6 * (32 − 1.5) * 12(4.45 * 25.4) = 248 × 10^3 mm^3 (2196 kip-in.)
L' = max{0.707 * 29, 16.5}(25.4) = 521 mm (20.50 in.)
DB/L' = 16.5/20.50 = 0.8049 1 − DB/L' = 0.1951
Midspan moment
= 2,196/4/0.8049^2{0.25 − 0.1951/3 + 0.1951^4/12}(4.45 * 25.4) = 17.7 × 10^3 kN-mm (156.8 kip-in.)
β = {157.6 − 21.85(27/16.5) − 0.3300(29/2.25) − 259.3(16.5/27) − 48.13[(27) (2.25)/16.5/(27 − 16.5)]$^{1/2}$ + 194.6(16.5/27)^2 + 127.4(2.25/29) − 21.65(16.5/29)}/1.080 = 0.8070
Equivalent section modulus
= 0.8070(29 − 16.5) * 2.25^2/12(25.4)^3 = 69.7 × 10^3 mm^3 (4.26 in.^{3})
Maximum bending stress
= 156.8/4.256(6.9) = 254 MPa (36.84 ksi) < 319 MPa (46.2 ksi) OK.

For maximum shear stress under parallel loading,

M/2 = 6 * (32 − 1.5) * 12/2(4.45 * 25.4) = 124 × 10^3 kN-mm (1,098 kip-in.)
b = min{0.707 * 29, 16.5}(25.4) = 419 mm (16.5 in.)
b/T = 7.333 C' = 0.301
γ = {210.0 − 66.9(29/16.5) − 0.1719(29 − 16.5)/2.25 − 714.8(16.5/27) + 358.3(16.5/27)^2 − 48.16[27 − 0.707(29)]/(27 − 16.5) − 288.2(29 − 16.5)/(1.414(27) − 16.5) + 381.0(29/27)}/1.094 = 1.545
Equivalent torsional section modulus = 1.545(0.301) 16.5(2.25^2)(25.4)^3 = 637 × 10^3 mm^3 (38.85 in.^{3})
Maximum shear stress = 1,098/38.85(6.90) = 195 MPa (28.28 ksi) ≈ 193 MPa (28 ksi) OK.

The experience of several such redesigned examples for deficient existing poles shows that increasing the base-plate thickness is most effective in reducing the stress level in the base plate.

CONCLUSIONS

In general, both the diagonal and parallel loadings should be considered as critical loading cases in designing signal poles. Current AASHTO analysis methods for the post and the anchor bolts appear to be appropriate on the basis of the load test results. A semiempirical analysis method for the base plate is suggested that decomposes the base plate into three simple components for respective critical stresses under the two critical loadings. This method presents clear mechanical origins of the stress concentration simply and is based on FEA of 28 poles with modelings verified by five full-scale load tests. Hand calculation is sufficient for its design applications.

ACKNOWLEDGMENTS

FHWA provided partial support for this study. The cooperation of G. Scaife and the staff of Carlan Manufacturing Company, Long Island, New York, for the load testing is appreciated. Many New York Department of Transportation personnel made the completion of this study possible. Special thanks are due to L. N. Johanson for his comments in the course of this study; D. M. Berkley, W. J. Deschamps, E. W. Dillon, M. J. Gray, G. L. Howard, and J. Lall for their assistance in the testing and FEA; and I. A. Aziz, A. D. Emerich, and D. L. Noonan for their assistance in preparing the figures and editing.

REFERENCES

1. *Standard Specifications for Structural Supports for Highway Signs, Luminaires and Traffic Signals*. AASHTO, Washington, D.C., 1985.
2. *Method for Calculating the Loads Applied to Span Wire Traffic Signal Poles*. Engineering Instruction EI83-38. Facilities Design Division, New York State Department of Transportation, Albany, Sept. 14, 1983.
3. *CASA/GIFTS User's Reference Manual*. Software Package Version 6.4.3. CASA/GIFTS, Inc., Tucson, Ariz., Oct. 1989.
4. S. J. Boulos, G. Fu, and A. Alampalli. *Testing, Analysis, and Design of Steel Traffic Signal Poles*. Final Report. New York State Department of Transportation, Albany, Dec. 1992.
5. F. P. Beer and E. R. Johnston. *Mechanics of Materials*. McGraw-Hill, New York, 1981.

Publication of this paper sponsored by Committee on General Structures.